Wing mass estimation algorithm for medium range box wing aircraft

P. O. Jemitola
p.o.jemitola@cranfield.ac.uk
G. Monterzino and J. Fielding
Department of Aerospace Engineering
Cranfield University
Cranfield, UK

ABSTRACT

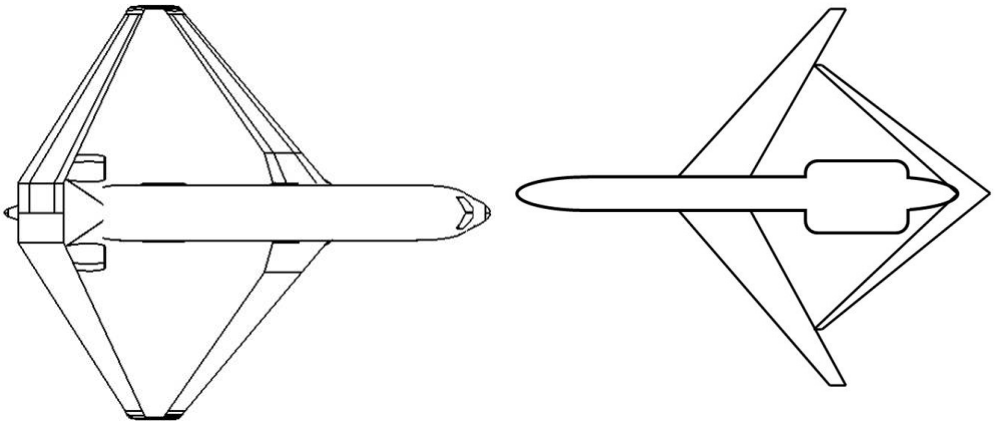
A procedure for defining an empirical formula for the mass estimation of the fore and aft wings field Uof a medium range box wing aircraft is described. The procedure is based upon the work of Howe for estimating the wing mass of conventional cantilever wing aircraft. The paper outlines the procedure used to relate conventional cantilever wings to box wing aircraft wings. Using a vortex lattice tool, finite element methods and regression analysis, the modification performed on the coefficient in Howe's method to enable its use on a medium range box wing aircraft is outlined. The results show that the fore and aft wings would use the same correction coefficient and that the aft wing would therefore be lighter than the fore wing on a medium range box wing aircraft.

NOMENCLATURE

AWTM	aft wing torsion box mass
b	span
C_1	mass coefficient
FEA	finite element analysis
FWTM	fore wing torsion box mass
MTOM	maximum take-off mass

Paper No. 3776. Manuscript received 12 October 2011, revised version received 11 March 2012, accepted 3 May 2012.

https://doi.org/10.1017/S0001924000008022 Published online by Cambridge University Press



(a) Box wing (b) Joined wing

Figure 1. Unconventional aircraft configurations.

M_W	wing mass
N	normal acceleration factor
S	wing area
V_D	design diving speed
τ	average thickness to chord ratio
$\Lambda_{1/4}$	quarter chord sweep angle
λ	taper ratio

Subscript

B	box
C	cantilever

1.0 INTRODUCTION

There are renewed interests in unconventional designs as part of the search for the next future airliner configuration. Configurations such as the box wing and joined wing, Fig. 1, have been studied by Wolkovitch[1], Kroo[2], Nangia[3] and Henderson[4]. Their studies show the higher stiffness and lower induced drag of the box and joined configurations and hence their potential of improved fuel efficiency and reduced direct operating costs.

Biplane configurations, from which the box wing is derived, were studied by Prandtl[5], Munk[6] and recently Frediani[7]. They all highlight the superior aerodynamic efficiency of biplane designs over conventional configurations. Although box and joined wing aircraft are frequently referred to as the same the configurations and principles of operation are different. This study is not on the classical joined wing configuration shown in Fig. 1(b) but on the box wing aircraft shown in Fig. 1(a) which is based on Prandtl's[5] best wing system where both wings produce equal lift forces. The box wing aircraft configuration and principle of operation has already been successfully flight tested by Frediani[8] with results that are in accordance with the mathematical model.

https://doi.org/10.1017/S0001924000008022 Published online by Cambridge University Press

However, one of the challenges in the conceptual design of a box wing airliner is estimating the wing mass component of the overall aircraft mass. An aircraft's mass needs to be reasonably estimated at the conceptual design phase for several reasons including the direct relationship between an aircraft's operating empty mass, the aircraft's price and direct operation cost[9]. This relationship is even more paramount for novel designs where conventional mass estimation methods may not apply. Several empirical formulae exist for estimating the mass of conventional cantilever wings such as those given by Jenkinson[9], Raymer[10] and Torenbeek[11] but these would be misleading if applied directly to an unconventional configuration such as box wing aircraft. The study by Miura *et al*[12] on parametric weight evaluation of joined wings by structural optimisation was aimed at presenting trends and not development of a wing mass estimation algorithm. Furthermore, the trends presented cannot be applied to box wing configurations as their study relates to classical joined wing aircraft (Fig. 1(b)) only.

Wing mass estimation algorithms are especially useful when quick approximate answers are needed during preliminary investigations; such answers indicate trends without the necessity of detailed knowledge of the aircraft. For the box wing aircraft, so far, there are no empirical formulae for estimating wing mass. A practical approach for developing a formula for use at the early conceptual design stage would be to modify an existing algorithm by determining the appropriate coefficients for the fore and aft wings. To be of use such an algorithm must include all the variable parameters which influence the answer and must not be too complex or require detailed knowledge of the design. Torenbeek's[11] method requires many factors not available at the early conceptual design stage, so does Jenkinson's[9] method as well. The main drawback with Raymer's[10] method at the early design stage is that it requires knowledge of the wing control surface area. In contrast, Equation (1)[13], which is for conventional cantilever aircraft, requires parameters usually available at the early design stage. Equation (1) is based on Howe's[14] equation and he states its accuracy as 86%; a value which can be considered acceptable for the conceptual design stage.

$$M_W = C_1\left[\frac{bS}{\mathrm{Cos}\Lambda_{1/4}}\left(\frac{1+2\lambda}{3+3\lambda}\right)\left(\frac{M_{TOM}N}{S}\right)^{0{\cdot}3}\left(\frac{V_D}{\tau}\right)^{0{\cdot}5}\right]^{0{\cdot}9} \quad \ldots (1)$$

Equation (1) is a consequence of the analysis of one hundred aircraft of all types. Its derivation involved computing the optimised minimum mass of the wing primary structure by using equations based on the bending and torsional strengths which were theoretically required. Subsequently, the computed optimal mass was modified by making allowances for departure of the structural concept from the optimum. The component of the wing mass which ensures adequate torsional stiffness and prevents flutter is substantiated by the design diving speed that appears in Equation (1).

Furthermore, the mass of secondary items such as high lift devices and controls, were estimated using statistical data. The algorithm is intrinsically a compromise between wing stiffness and lightness and is based on the use of aluminium alloy construction. There isn't an inertia relief factor in the equation but it is implicitly accounted for in the values of the coefficient C_1. The algorithm also uses C_1 to account for different types of aircraft and layout details therefore suiting the purpose for a box wing estimation algorithm. Some values of C_1 given in the Aircraft Mass Prediction[13] manual are shown in Table 1. Thus, Equation (1) is suitable for use in developing a wing mass estimation algorithm for box wing aircraft. What has to be determined is the value of C_1 that would apply to the fore wing and that for the aft wing of a medium range box wing aircraft.

https://doi.org/10.1017/S0001924000008022 Published online by Cambridge University Press

Table 1
Aircraft type mass coefficients

Aircraft type	C_1
Long range	0·082
Short range	0·034
Braced wing	0·021
Light aircraft	0·028-0·034

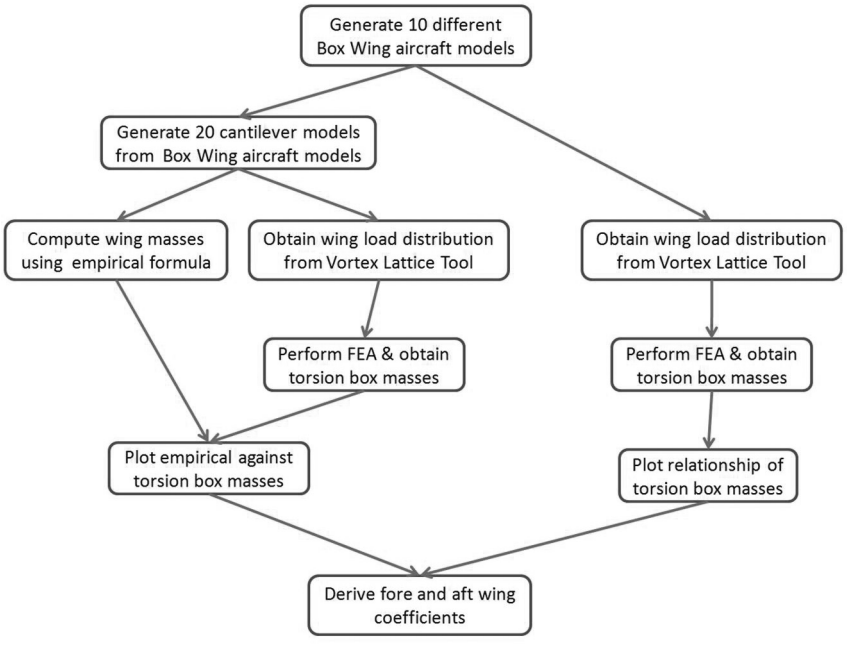


Figure 2. Procedure schematic.

2.0 REFERENCE AIRCRAFT DESCRIPTION

This work derives from a previous conceptual design of a medium range box wing aircraft studied in Cranfield University and is outlined in Smith and Jemitola1[5]. It is a 4,000nm range box wing airliner with a maximum takeoff mass of 127,760kg and wing span of 37·6m. The fore and aft wing gross areas are 118·32m^2 each, while the sweep angles are 40 and –25 degrees respectively. Overall fuselage length is 46 metres and maximum diameter 5·6m.

3.0 COEFFICIENT DERIVATION PROCEDURE

The procedure to determine the coefficient C_1 of Equation (1) for the box wing aircraft is outlined in Fig. 2. Ten different box wing aircraft models with appropriate medium range wing parameters were generated by considering a wide range of wing parameters in order to expand the applicability of the coefficient being developed. Thus, the parameters chosen represented the three extremes of the spectrum under consideration and eight other points between these extremes as

https://doi.org/10.1017/S0001924000008022 Published online by Cambridge University Press

Model	S (m^2)	λ	b (m)	τ	Fore Wing Sweep (^{o})	Aft Wing Sweep (^{o})
Box 1	112	0.27	32	0.09	30	-19
Box 2	117	0.26	33	0.09	31	-20
Box 3	110	0.25	33	0.09	32	-22
Box 4	115	0.28	33	0.10	33	-24
Box 5	120	0.27	34	0.11	30	-26
Box 6	122	0.26	34	0.11	33	-28
Box 7	118	0.25	35	0.12	35	-18
Box 8	116	0.25	34	0.12	33	-20
Box 9	124	0.25	35	0.13	32	-22
Box 10	119	0.25	34	0.13	29	-24

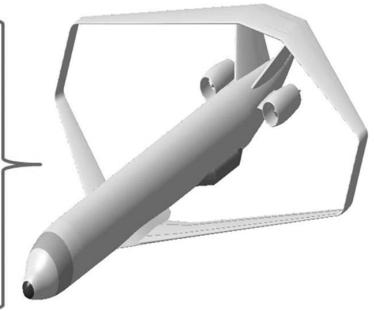


Figure 3. Box wing model parameters.

Model	S (m^2)	λ	b (m)	τ	Sweep (^{o})
AS 1	112	0.27	32	0.09	30
AS 2	117	0.26	33	0.10	31
AS 3	110	0.25	33	0.11	32
AS 4	115	0.28	33	0.12	33
AS 5	120	0.27	34	0.10	30
AS 6	122	0.26	34	0.11	33
AS 7	118	0.25	35	0.12	35
AS 8	116	0.25	34	0.12	33
AS 9	124	0.25	35	0.13	32
AS 10	119	0.25	34	0.13	29

Model	S (m^2)	λ	b (m)	τ	Sweep (^{o})
FS 1	112	0.27	32	0.09	-19
FS 2	117	0.26	33	0.09	-20
FS 3	110	0.25	33	0.09	-22
FS 4	115	0.28	33	0.10	-24
FS 5	120	0.27	34	0.11	-26
FS 6	122	0.26	34	0.11	-28
FS 7	118	0.25	35	0.12	-18
FS 8	116	0.25	34	0.12	-20
FS 9	124	0.25	35	0.13	-22
FS 10	119	0.25	34	0.13	-24

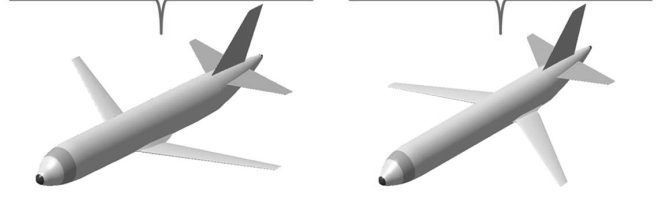


Figure 4. Cantilever wing model parameters.

shown in Fig. 3. The wing parameters of the ten box wing models were subsequently used to generate 20 cantilever winged (ten forward swept and ten aft swept) aircraft models shown in Fig. 4. The masses of these wings were then estimated using Equation (1). Next, each of the 20 cantilever winged aircraft was modelled in a vortex lattice tool to obtain the wing load distribution for an assumed flight condition.

The wing load distributions, including the contributions to torsion coming from the aerofoil section properties and the moment arm between the lift application point and the elastic axis of the torsion box were obtained from a vortex lattice analysis tool called Athena Vortex Lattice (AVL)[16]. AVL is a program that utilises vortex-lattice theory for aerodynamic and dynamic analysis of a given aircraft geometry. It uses a vortex lattice model for the lifting surfaces, together with a slender-body model for fuselages and by simulating the flow field it predicts the pressure distribution around the simulated body.

https://doi.org/10.1017/S0001924000008022 Published online by Cambridge University Press

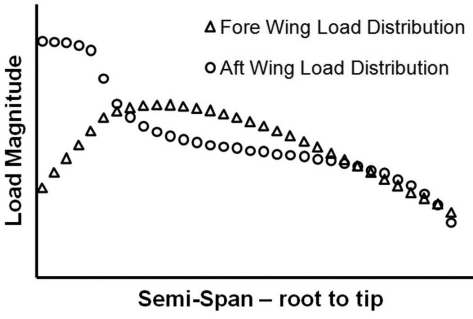


Figure 5. Box wing load distribution.

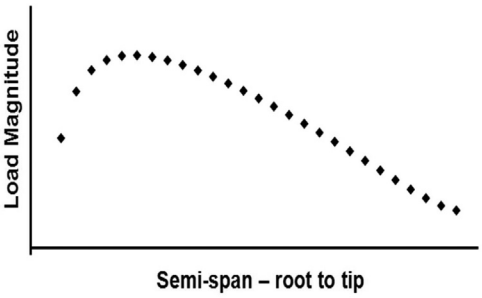


Figure 6. Cantilever wing load distribution.

The wing loads were then used to perform FEA on the torsion box models of the entire cantilever winged aircraft from which the torsion box masses were obtained. A relationship was subsequently established between the empirical and torsion box masses of the 20 cantilever wing aircraft. In a similar manner the ten box wing models were modelled in a vortex lattice tool to obtain the wing loads and distribution for an assumed flight condition. The wing loads were then used to perform FEA on the torsion box models of the box wing aircraft from which their masses were obtained. A relationship was thereafter plotted with the equivalent cantilever torsion box model mass and that of the box wing. From these plots the coefficients for the fore and aft wings were derived.

4.0 AIRCRAFT MODEL PARAMETERS

For the box wing aircraft models MTOM = 127,760kg and for the cantilever aircraft MTOM = 63,880kg. All models were designed for a 3,500nm range. Other model parameters are shown in Figs 3 and 4.

5.0 AERODYNAMIC LOADS

Figures 5 and 6 show the load distributions for the box and cantilever wings obtained from AVL. The effect of the fuselage on the lift distribution was accounted for by implementing 40% of the root chord at the center line of the model as given in Howe[17].

The load condition assumed was a 2·5g manoeuvre case limit load at sea level at design diving speed, V_D, at maximum take-off weight. In a final design analysis, other loading conditions should also be examined, which include various possible combinations of control deflections and gust loadings. However, the conditions that were assumed in this preliminary study are considered adequate.

6.0 FINITE ELEMENT MODEL DESCRIPTION

Due to the simplicity of the torque box and elastic axis beam type models used for the stress/strain analysis, only general stress trends were analysed. These trends were determined as a function of the beam span as opposed to a plane stress or shear flow analysis which would also estimate the stresses around the torque box. Furthermore, as a first approximation only a linear analysis was conducted.

https://doi.org/10.1017/S0001924000008022 Published online by Cambridge University Press

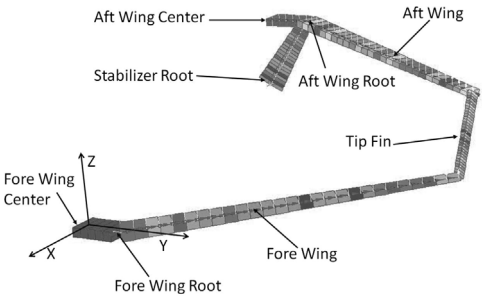


Figure 7. Box wing structural mode.

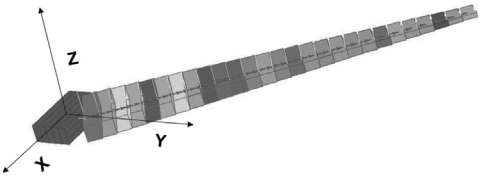


Figure 8. Cantilever wing structural model.

Strand7[18] was used for the finite element analysis. The Strand7 model consists of any number of structural elements connected by a common control point grid. Several different Strand7 elements could be used to model an aircraft wing. Only beam, plate and brick elements were considered for the finite element models. The beam element was chosen for the models because of the enormous gain in simplicity over a plate or brick model. Beam elements have two nodes at their ends and the single dimension is length. Other dimensions can be specified from a range of beam sections available thereby giving three-dimensional properties. In its most general form the beam element can carry axial force, shear force, bending moment and torque. The beam element can also be used to simulate a bar with a non-uniform cross section by interpolating sections. Strand7 has the capability of applying distributed or concentrated loads to a beam element. It also can apply distributed or point torque or moment on beam elements.

Since the wing configuration analysed in this report is non-uniform (having taper, dihedral and sweep angle), the beam element provides a more practical wing model as opposed to a brick or plate element. Figures 7 and 8 present a beam version of the wing models. As the analysis targets conceptualists rather than structural analysts the fuselage is omitted from the idealisation but accounted for by the boundary conditions imposed on the model. Wing inertia relief was ignored because its presence or absence was not going to affect the trends observed. In addition, the analysis was conducted with all models in iso-inertia conditions (equal to zero). Due to the symmetric nature of the torsion box model, the elastic axis and geometric centres of the wing models coincide and it was along this axis that the loads were applied. For this reason forces and moments are transmitted through the wing tip joints (a single grid point) by equating the respective translations and rotations of the joint receivers at the joint. The global co-ordinate system used for static analysis is defined in Figs 7 and 8.

7.0 WING CROSS SECTION PROPERTIES

Studies by Wolkovitch[1] indicate that the optimum wing torsion box cross-sectional profile of the box wing configuration is one which accounts for the tilted bending axis of the wings by having the 'bending-resistant material' concentrated near the upper leading edges and lower trailing edges as shown in Fig. 9. However, for simplicity, an idealised wing torsion box cross-sectional geometry, illustrated in Fig. 10, was used in this study. Although this is not the optimum torsion box cross section for a box wing, it was assumed to be adequate for the present study. Furthermore, since the wing cross sections are perpendicular to the wing's elastic axis, the root and tip of the swept wings create modelling problems. However, for slender swept wings and applied loads

https://doi.org/10.1017/S0001924000008022 Published online by Cambridge University Press

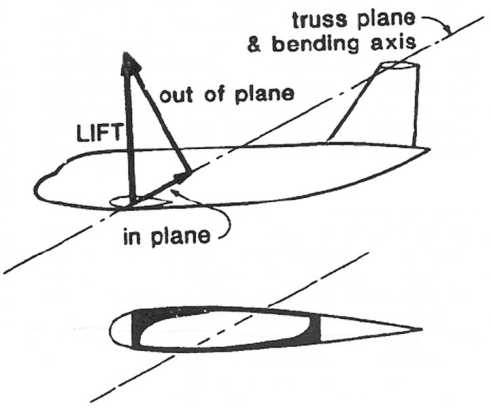


Figure 9. Box wing tilted bending axis[1].

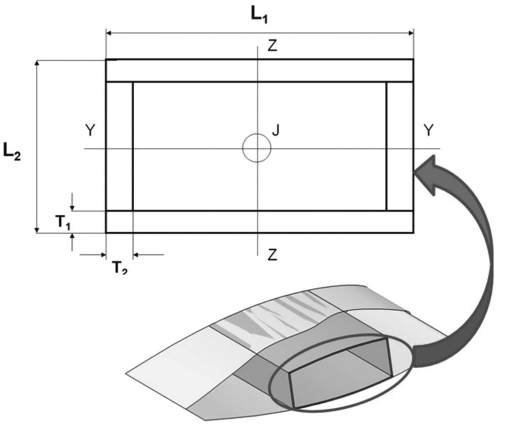


Figure 10. Idealised torsion box cross-section geometry.

through the wing elastic axis, an effective wing root and tip may be assumed, simplifying the wing finite element model.

The specific aerofoil sections used in this study were not required due to the conceptual nature of the analysis although Wolkovitch[1] has highlighted the suitability of box wings for thin aerofoils. In addition, the torsion boxes for all finite element models were assumed to occupy 50% of the chord.

Strand7[18] beam elements require cross sectional properties as program inputs and automatically compute properties such as wing cross sectional area A, the second moments of area Iyy and Izz, and the polar second moment of area, J. Note that for a symmetrical cross section, $Iyz = 0$. The material properties used for all the finite elements are those of aluminium alloy 2024 - T42 selected from the Strand7 material database; modulus of elasticity E = 73·0GPa, modulus of rigidity G = 27·6GPa, density ρ = 2,770kg/m^3.

8.0 STRUCTURAL SIZING AND FEA PROCEDURE

Sizing was done by implementing the algorithms outlined in Howe[17]. Stiffness criteria that ensure adequate wing aero-elastic performance was accomplished following Howe's approach. The idealised wing structural box model used for the finite element analysis makes the distributed flange construction method ideal for sizing the torsion box skin and web, T_1 and T_2 in Fig. 9.

The torsional loads from the aerofoil section properties and from the moment arm between the lift application point and the elastic axis of the torsion box were combined to generate an equivalent torque applied along the elastic (and geometrical) axis of the torsion box. By superposition principle, said equivalent torque and the lift load (applied along the elastic axis as well) were considered together to achieve a representative FEA model of the physical system.

The structural sizing and FEA procedure for each model included development of a three-dimensional model of the port wing torsion box assembly in Strand7[18] with an initial pooling set of values for T_1 and T_2 obtained from historical data. The loads obtained from AVL were then applied in a distributed manner along the elastic axis of the wings. Thereafter, a linear analysis was performed. A second finite element model of the same wing was then built but with the results of the previous linear analysis implemented in T_1 and T_2. Distributed loads from AVL were then

https://doi.org/10.1017/S0001924000008022 Published online by Cambridge University Press

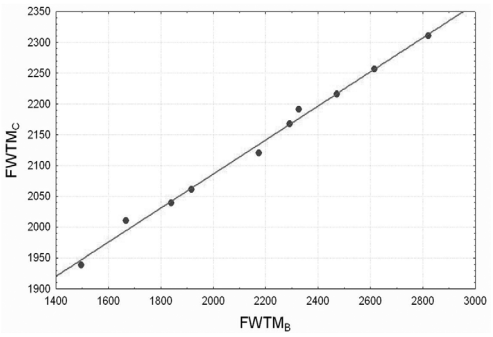


Figure 11. Cantilever/box relationship.

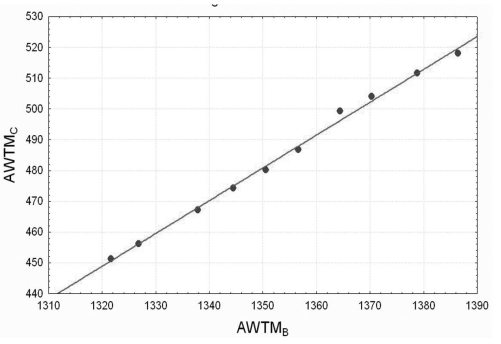


Figure 12. Cantilever/box relationship.

applied and another linear analysis performed with results obtained. These results were then implemented in a third model of the same wing and the procedure repeated until there was virtually no change in the model's T_1 and T_2 values. This state established the converged solution for that wing model and the mass was thereafter obtained from Strand7. This procedure was performed for all wing models.

9.0 RESULTS AND COEFFICIENT DERIVATION

The results of the outlined procedure were used to perform a regression analysis and their R_2 and p-values determined. R_2 is the proportion of variability in a data set that is accounted for by a statistical model[20]. It provides a measure of how well future outcomes are likely to be predicted by a model. The P value answers this question: If there were no linear relationship between X and Y overall, what is the probability that randomly selected points would result in a regression line as far from horizontal (or further) with respect to what you observed?[21]. In other words the p-value gives the probability of obtaining a test statistic as large as the one calculated from data, if in fact the true slope is zero. Thus, the smaller the p-value the more significant the regression. Customarily, if the p-value is below 0·05 the regression is significant[22]. Plots of the torsion box masses of the cantilever wings and their equivalent box wing aircraft wing are shown in Figs 11 and 12. Figure 11, which is a plot of the cantilever wing against the equivalent fore wing of the box wing aircraft model gives a coefficient of determination R_2 of 0·9938 and a p-value of $p = 4{\cdot}00 \times 10^{-10}$ showing that the regression is significant. For the aft wing, analysis gives a gives a coefficient of determination R_2 of 0·9960 and a p-value of $p = 7{\cdot}05 \times 10^{-10}$ (see Fig. 12), again showing a high linear correlation. Thus, the relationship between the wings as cantilevers and as part of the box wing arrangement is significant.

The empirical masses of the cantilever wings were computed using Equation 1. A plot of these empirical masses against their finite element model torsion box masses gave the plot in Fig. 13. The analysis gives a coefficient of determination R_2 of 0·9907 and a p-value of $p = 2{\cdot}09 \times 10^{-9}$ showing the high linear correlation.

The above procedure for the aft wings is shown in Fig. 14. The regression has a coefficient of determination R_2 of 0·9946 and a p-value of $p = 2{\cdot}33 \times 10^{-10}$ showing that the regression fits the points very well. It also means each individual variable has a high linear correlation with the dependent variable. The quality indicators for all analyses are shown in Table 2.

https://doi.org/10.1017/S0001924000008022 Published online by Cambridge University Press

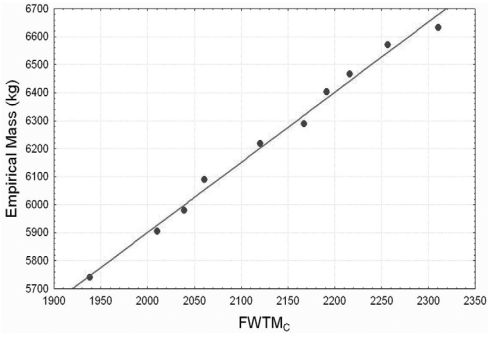


Figure 13. Empirical/FEA relationship.

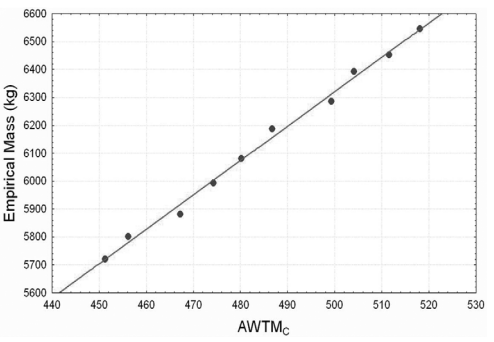


Figure 14. Empirical/FEA relationship.

Table 2
Regression quality indicators

Analysis	*p* value	R_2	Adjusted R_2
Fig. 11	$4{\cdot}00 \times 10^{-10}$	0·9938	0·9931
Fig. 12	$7{\cdot}05 \times 10^{-10}$	0·9960	0·9955
Fig. 13	$2{\cdot}09 \times 10^{-9}$	0·9907	0·9895
Fig. 14	$2{\cdot}33 \times 10^{-10}$	0·9946	0·9939

The key to developing a coefficient for estimating box wing aircraft wing mass lies in establishing a relationship between the empirical masses of the cantilever wings and the results of the FEA carried out. To this end, a relationship was established between the mass of the torsion boxes of the wings as part of a box wing arrangement ($FWTM_{B)}$ and the mass of the wings as cantilevers ($FWTM_C$). This relationship for the fore wing is given as:

$$FWTM_C = 0{\cdot}2765 FWTM_B + 1{,}533 \quad \ldots (2)$$

The relationship between the empirical mass of the fore wing as a cantilever and its torsion box mass is given as:

$$M_W = 2{\cdot}5159 FWTM_B + 870{\cdot}96 \quad \ldots (3)$$

Thus, by substitution, the empirical mass of the wing as part of the box wing arrangement is given by:

$$M_W = 2{\cdot}6956 FWTM_B + 4{,}727{\cdot}83 \quad \ldots (4)$$

Relating this equation to Equation (1) gives:

$$0{\cdot}6956 FWTM_B + 4737{\cdot}83 = C_1 \left[\frac{bS}{\mathrm{Cos}\Lambda_{1/4}} \left(\frac{1+2\lambda}{3+3\lambda} \right) \left(\frac{M_{TOM} N}{S} \right)^{0{\cdot}3} \left(\frac{V_D}{\tau} \right)^{0{\cdot}5} \right]^{0{\cdot}9} \quad \ldots (5)$$

Solving this equation for the fore wing of Box 1 model gives a coefficient $C_1 = 0{\cdot}028$.

https://doi.org/10.1017/S0001924000008022 Published online by Cambridge University Press

The values of C_1 for other fore wing models gives an approximated value of 0·028. With the average being 0·028 and the variance $2{\cdot}51 \times 10^{-8}$.

The above process was also repeated for the aft wing. Here as well the average coefficient obtained is 0·028 and the variance $2{\cdot}54 \times 10^{-8}$.

Thus, the empirical wing mass estimation equation for the fore and aft wings of a medium range box wing aircraft can be written as:

$$M_W = 0{\cdot}028\left[\frac{bS}{\mathrm{Cos}\Lambda_{1/4}}\left(\frac{1+2\lambda}{3+3\lambda}\right)\left(\frac{M_{TOM}N}{S}\right)^{0{\cdot}3}\left(\frac{V_D}{\tau}\right)^{0{\cdot}5}\right]^{0{\cdot}9} \quad \ldots (6)$$

10.0 CONCLUSION

The objective of this paper was to determine a value for the type coefficient of an existing weight estimation method (Equation (1)) applicable to medium range box wing aircraft. As the name suggests, the coefficient can account for the sort of aircraft that is being analysed, such as long range, short range, braced wing, etc (see Table 1). The wing mass estimation coefficient of 0·028 derived for the fore wing proved to be the same as that derived for the aft wing. As the wings carry the same load and are connected by tip fins it was anticipated that their coefficient may be the same. Also, the wings are mutually bracing each other, the same set of constraints being applied to both. The significance of the fact that the fore and aft wing mass estimation coefficients are the same is that the aft wing of a medium range box wing aircraft would be lighter than the fore wing. The reason for this is that for a medium range box wing aircraft the sweep angle of the aft wing would typically be less than that of the fore wing (wing area being the same), the resulting mass of the aft wing would be bound to be lower. This general result is of significant importance to the conceptual designer, for this difference in mass would be of consideration for centre of gravity and static margin issues of the configuration. The mass difference would also be of influence in the positioning of other heavy items such as engines and landing gears.

The analytic models used for this study were relatively simple to reduce the data preparation and the turn-around time of data processing. Also, the weights estimated obtained from Strand7 in this study are limited to the structural torsion box of the wing; trailing and leading edges, control surfaces and auxiliary component weights were excluded. Thus, for more detailed analysis further studies would be required which should include torsion box cross-sections that account for the tilted bending axis of the box wing configuration.

ACKNOWLEDGEMENTS

The authors acknowledge the support of the Department of Aerospace Engineering, Cranfield University.

REFERENCES

1. WOLKOVITCH, J. The joined wing: An overview, *J Aircr*, March 1986, **23**, pp 161-178.
2. KROO, I., GALLMAN, J.W. and SMITH, S.C. Aerodynamic and structural studies of joined-wing aircraft, *J Aircr* 1991, **28**, (1), pp 74-81.
3. NANGIA, R.K., PALMER, M.E. and TILMAN, C.P. Unconventional high aspect ratio joined-wing aircraft with aft and forward swept wing tips, January 2003, AIAA-2003-0605, 41st Aerospace Sciences Meeting, Nevada, USA.

https://doi.org/10.1017/S0001924000008022 Published online by Cambridge University Press

4. HENDERSON, W.P. and HUFFMAN, J.K. Aerodynamic characteristic of a tandem wing configuration at a Mach number of 0·30, March 1975, Report TM X-72779, NASA.
5. PRANDTL, L. Induced drag of multiplanes, 1924, Technische Berichte, **III**, (7).
6. MUNK, M. *The Minimum Induced Drag of Airfoils*, March 1923, Report 121, NACA.
7. FREDIANI, A. The Prandtlwing, Lecture series on innovative configurations and advanced concepts for future civil aircraft, 2005, Von Karman Institute, VKI 2005-06.
8. FREDIANI, A., RIZZO, E., CIPOLLA, V., CHIAVACCI, L., BOTTONI, C., SCANU, J. and IEZZI, G. Development of ULM Prandtlplane aircraft and flight tests on scaled models, 2007, XIX Congresso Nazionale AIDAA, September 2007, Milan, Italy.
9. JENKINSON, L, SIMPKIN, P. and RHODES, D. *Civil Jet Aircraft Design*, 2001, Arnold Publishing, London, UK.
10. RAYMER, D.P. *Aircraft Design: A Conceptual Approach*, 1992, AIAA, Washington, DC, USA.
11. TORENBEEK, E. *Synthesis of Subsonic Airplane Design*, 1982, Delft University Press, Delft, The Netherlands.
12. MIURA, H., SHYU, A. and WOLKOVITCH, V. Parametric weight evaluation of joined wings by structural optimization, 1985, AIAA/ASME/ASCE/AHS 26th Structures, Structural Dynamics amd Materials Conference, FL, USA, April 1985.
13. HOWE, D. DAeT 9317 — Aircraft mass prediction, 2009, Department of Aerospace Engineering, Cranfield University.
14. HOWE, D. The prediction of aircraft wing mass, Proceedings Institution of Mech Engineers, Part G, *J Aerospace Eng*, April 1996, **210**, (G2), pp 135-145.
15. SMITH, H. and JEMITOLA, P. A-9 box wing medium range airliner — Project specification, 2009, Department of Aerospace Engineering, Cranfield University, UK.
16. DRELA, M. and YOUNGREN, H. Athena Vortex Lattice User Manual, Version 3.26, 2006, http://web.mit.edu/drela/Public/web/avl/.
17. HOWE, D. *Aircraft Loading and Structural Layout*, 2004, Professional Engineering Publishing, London, UK.
18. Strand7, Release 2.3.8 User's Guide, 2007, Strand7 Pty Ltd.
19. HOWE, D. *Aircraft Conceptual Design Synthesis*, 2001, Professional Engineering Publishing, London, UK.
20. STEEL, R.G.D. and TORRIE, J.H. *Principles and Procedures of Statistics*, 1960, McGraw-Hill, New York, USA.
21. MOTULSKY, H. and CHRISTOPOULOS, A. *Fitting Models to Biological Data using Linear and Nonlinear Regression*, 2004, Oxford University Press, New York, UK.
22. MEHNEN, J. *Linear Regression*, 2011, Doctoral Training Centre, Cranfield University, Cranfield, UK.

https://doi.org/10.1017/S0001924000008022 Published online by Cambridge University Press